Spacecraft Charging: Environment-Induced Anomalies

Alan Rosen*
TRW Systems, Rendondo Beach, Calif.

Large potential differences and accompanying arc discharges between various parts of a spacecraft may arise as a result of geomagnetic substorms. A large number of electronic malfunctions and other miscellaneous aberrations in the operation of spacecraft subsystems have been attributed to the substorm phenomenon. This paper reviews some of the substorm related operational problems experienced by synchronous altitude spacecraft systems, discusses the interaction of spacecraft with the substorm plasma environment, and presents the results of spacecraft charging model calculations. The effects of geomagnetic substorms on the design of spacecraft, especially questions relating to the choice of surface conductivities, concepts of spacecraft "ground," and shielding requirements are also discussed.

Introduction

ANOMALOUS behavior of unmanned satellites in geosynchronous orbits has been observed on many occasions. These generally consist of spontaneous, unpredictable switching commands, subsystem gain changes, firing of sensors, damage to subsystems, and, on rare occasions, the catastrophic loss of a satellite. The housekeeping data, which are generally available on most operational spacecraft, have not provided an effective diagnostic for explaining these events. However, a large body of indirect evidence is now available that leads to a definitive explanation of many of the observed malfunctions.

The general conclusion reached as a result of many previous studies and analyses[1-8] was that the space environment, particularly at synchronous altitudes, can cause a spacecraft to charge up differentially to the 20 kV range. This may lead to voltage breakdown or vacuum arcing, since many materials cannot withstand such high voltage stresses. The resulting electromagnetic interference (EMI) is induced into various spacecraft circuits, which may lead to triggering of integrated circuit switches, multivibrators, and one shots. Cases of irrepairable damage or total burnout of sensitive semiconductor components have also been observed as a result of environmentally generated EMI. In addition, the arcing phenomenon has given rise to degradation of thermal blankets (by vaporizing or burning the vacuum deposited aluminum present on the blanket), contamination of surfaces by vaporization products, triggering of light-sensitive devices, and anomalous functioning or failure of equipment (e.g., pressure transducers).

First, a review of the theory of spacecraft charging and the characteristics of the environment will be presented. This will be followed by an outline of some of the environmentally related operational problems experienced by synchronous altitude spacecraft and discussion of the evidence showing that these are of an environmental origin.

Space Plasma Effects

An overview of the theoretical considerations of the plasma-charging phenomena is presented here. For a more complete description the reader is referred to Refs 2, 9-12. A spacecraft in the space environment is immersed in a plasma of variable temperature and flux density. In the steady state, every part of the spacecraft will come into electrical equilibrium with the plasma by developing surface charges of the proper sign and magnitude so that the net current, represented by the deposition and release of charged particles from the surface, is zero. This surface charge tends to accelerate charges of one sign and slow down charges of the opposite sign so that a sheath of charge is formed around the spacecraft. The equilibrium potential of the surface of the spacecraft is the potential difference between the surface and the ambient plasma sheath.

The steady-state equilibration is a requirement that the sum of the various currents of charged particles to and from each surface element be equal to zero. The most important contributors to the equilibration currents are the primary plasma electron and ion arrival at the surface, and the photoelectrons released when sunlight illuminates the surface. However, the contributions of secondary electrons released from the surface, under primary ion or electron impact, and possible electron reattraction to the surface, may also be significant and must be considered in a complete analysis of the problem.

The simplified spacecraft charging theory is based on a number of approximations of the ambient environment and the spacecraft. First, it is assumed that the neutral ambient gas density is sufficiently small that the spacecraft-sheath charge is not significantly modified by collision process (the collisionless plasma regime). This is a good approximation of the environment at six Earth radii ($6R_e$). Other approximations relate to the temperature of electrons and ions T_e and T_p, the velocity distribution of the particles, the relative magnitudes of the contribution to the current of electrons J_e, ions J_p, photoelectrons $J_{\rm ph}$, RAM currents $J_{\rm RAM}$, and secondary emission $J_{\rm sec}$, and the geometry and material composition of the spacecraft. The partial current densities contributed by the incident electrons, protons and ejected photoectrons are [when the potential of the spacecraft, $\phi(x)=0$]

$$J_e{}^s \cong -N_e(kT_e/m_p)^{1/2} = -N_e e<v_e>$$

$$J_p{}^s \cong N_e(kT_p/m_p)^{1/2} = N_p e<v_p>$$

$$J_{\rm ph} = N_{\rm ph} e<v_{\rm ph}>$$

In the absence of photoemission $J_{\rm ph}=0$ and at equilibrium, a high negative potential of the spacecraft repels the lower energy electrons, so that only the higher energy electrons contribute to the current. If one integrates over the distribution curve, the fraction of electrons contributing to the current is

$$N/N_e = e<v_e> e^{-|e\phi|/kT_e}$$

Presented as Paper 75-91 at the AIAA 13th Aerospace Sciences Meeting, Pasadena, California, January 20-22, 1975; submitted February 12, 1975; revision received September 16, 1975. This work is a summary of research and studies performed by various groups at TRW Systems, AF-SAMSO organizations, Aerospace Corp., NASA laboratories, and universities. The support of G.T. Inouye, J.L. Vogl, and J.M. Sellen, Jr. of TRW Systems, and S.E. DeForest of the University of Alabama for innumerable discussions and for supplying much of the data is hereby acknowledged.

Index category: Earth Satellite Systems, Unmanned.

*Manager, Space Sciences Department. Member AIAA.

and the surface potential ϕ will be determined from

$$-N_p e<v_p>=e<v_e>N_e e^{-e\phi/kT_e}.$$

Solving for ϕ yields

$$\phi=kT_e/e \ln (J_e^s/J_p^s)$$

where $j^s=$ the initial current striking the surface before the accumulation of surface charge ($\phi=0$). Similarily, in the case of photoillumination, $j_p<<J_{ph}$, so that

$$\phi=-(kT_e/e) \ln (J_e^s/j_{ph}^s).$$

A differential potential, a potential difference between two adjacent surfaces on a spacecraft, may occur under conditions where there is a difference of illuminations between the two surfaces. Differences in material composition, the geometry of the surface, and possible anisotropic flux distributions also contribute to differential potentials. The occurrence of a high differential voltage is a more likely cause of RFI than the occurrence of a high spacecraft potential with respect to the ambient plasma. The capacitance of the spacecraft with respect to the ambient plasma is generally exceedingly small in comparison with the largest capacitance that may occur between adjacent surfaces. For example, large areas of a spacecraft may be covered with thermal blanket material consisting of 0.5-mil-thick mylar covered on one side with vacuum deposited aluminum approximately 2000 Å in thickness. The capacitance of one square meter of such a material, between adjacent aluminum surfaces, may be 10,000 times greater than the capacitance of the total spacecraft with respect to the plasma. The charge accumulation (and possible subsequent discharge current) is, therefore, potentially 10,000 times greater between the aluminum surfaces than between the spacecraft and the ambient plasma.

In general, two surfaces, not electrically connected, will charge to different potentials. In the Earth's ionosphere $kT_e \cong 1$ V or less and the potential difference between a dark and illuminated surface will be a few volts. In the Earth's radiation belt, the large flux of cold plasma ($kT_e<10$ V) dominates over the relatively small flux of high-energy trapped radiation, and the differential potential is low. In the local time sector from just before midnight to past dawn during a magnetic substorm a spacecraft at 3-10 R_e will be immersed in a hot plasma of energetic electrons ($kT_e \sim 5$-20 kV). In this environment spacecraft charging can range from zero to over 20 kV.

Magnetospheric Environment during Substorms

It is now common to view the magnetosphere either as being in a quiet state or as undergoing a substorm. Prior to the onset of a substorm, and provided that no substorm activity has occurred during a period of some tens of hours prior to the onset, the morning quadrant of the magnetosphere is filled with a cold (~ 1 eV) relatively dense ($n\sim$ 10 to 100 cm^{-3}) plasma. This cold plasma generally extends to the "trapping boundary" of electrons at value of $L \approx 8$, where L is the dipolar shell parameter defined by McIlwain[13] as $L=R/\cos^2 M$; R is in earth radii (R_e) and M is the geomagnetic (dipolar) latitude.

The temporal occurrence of substorm is an erratic one, since it depends on the unpredictable appearance of a southward component in the interplanetary magnetic field. There are often periods of several days during which little or no substorm is observed. However, it is somewhat more common to find substorms occurring in groups, spaced at 2-4-hr intervals, lasting for a few days (usually followed by a quiet period of a few days). Statistically speaking, it is an observationally based rule of thumb that substorm activity occupies on the order of 30%, and quiet periods some 70% of any given year. A geostationary satellite can, therefore, be expected to experience substorm effects for some 8-10% of its flight-time,

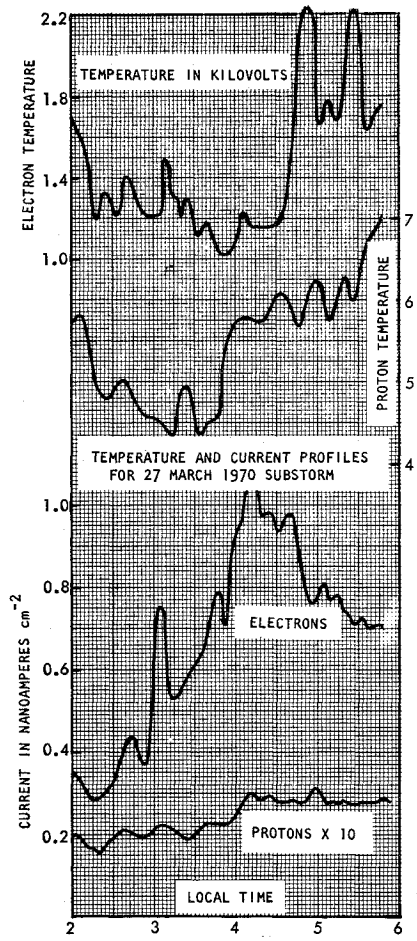

Fig. 1 Temperature and current profiles for electrons and protons, as measured on ATS-5 during substorms of March 27, 1970.

corresponding to its residence in the 2300 to 0700 local time segment of the magnetosphere.

Interaction of Spacecraft with Substorm Environment

It is possible to perform quantitative computations of the differential potential of a spacecraft or spacecraft component by use of a charging model. In this model the environment is represented by current generators that simulate the ambient environment plasma as a charging source, and the surface photoemission and secondary emission as a discharging source. The spacecraft configuration is represented by dielectric and metallic surfaces which collect charge from the environment by capacitive configurations associated with those surfaces and by geometrical/orbital parameters that determine which surfaces are and which are not exposed to sunlight. Both capacitors and spacecraft structure are fed by the current generators representing the environmental plasma and photoemission sources. The characterization of each current source tied to each part of the spacecraft depends on its area, it physical characteristics, and the environmental parameters. The diurnal and seasonal variation of exposed metallic surface areas for photoemission and the effects of internal cavities and apertures are both taken into account in the characterization of the capacitors and their associated current sources.

The equivalent current to a unit spacecraft area depends on the electron and proton flux, as well as the photoelectron and secondary electron emission from the surface. Representative values for electron and proton flux in synchronous orbit are available from measurements performed by DeForest and McIlwain[14,15] on ATS-5 and ATS-6.

Figure 1 shows the temperature and current profiles associated with the electron and proton fluxes observed

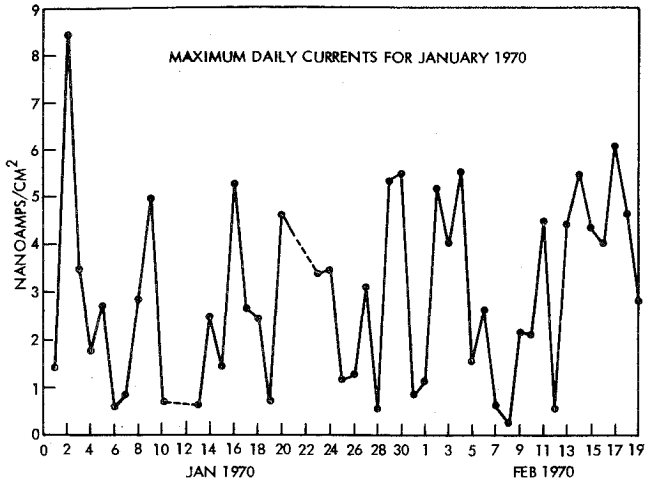

Fig. 2 Maximum daily currents for first 30 days of 1970, as measured on ATS-5.

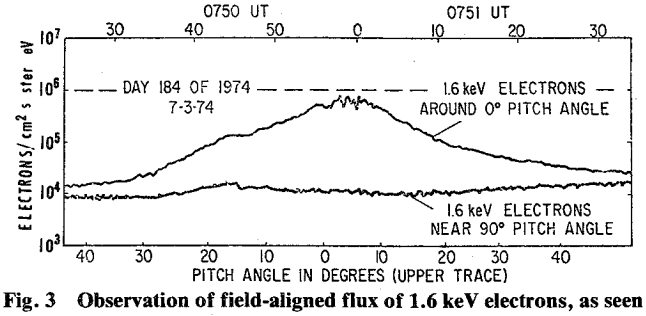

Fig. 3 Observation of field-aligned flux of 1.6 keV electrons, as seen on ATS-6.

during the substorm of March 27, 1970. The average energy per particle which is set equal to kT is obtained by dividing the energy flux by the particle flux (not shown in the figure). The peak electron temperature of 2.2 keV in Fig. 1 occurs 30-60 minutes after the peak electron current. DeForest believes that such behavior is typical. Also, the proton temperature is always higher than the electron temperature, averaging a factor of 2. The ratio of electron to proton current varies from 30 to 100 or greater. For a plasma in thermal equilibrium a factor of ≈ 43 (square root of proton to electron mass ratio) would be expected. Representative values of the equivalent electron and proton currents were deducted from ATS-5 data. Figure 2 shows a plot of the maximum measured daily currents for the first 30 days of 1970. For at least 24 hr on February 8 the current never exceeded 0.02 nA cm $^{-2}$, or more than a 40-fold increase, was attained. From Fig. 2 the average peak current during the 50-day period was ≈ 0.3 nA cm $^{-2}$, and the peak current was approximately 0.5 nA cm $^{-2}$.

The ATS-6 Satellite, launched in the summer of 1974, carried an improved version of the UCDS plasma detector of ATS-5. On ATS-6 the energy range was extended down to approximately 1 eV and a rotating platform was added that allowed more frequent observations of field-aligned fluxes.

The data analysis is still in a preliminary state, however, some of the more interesting results were presented at the AGU meeting in December 1974. Figure 3 shows an example of an observation of an intense field-aligned flux of electrons of 1.6 keV (courtesy, DeForest). The intensity of electrons in the loss cone, aligned with the geomagnetic field, is seen to be two orders of magnitude larger than the intensity perpendicular to the field. DeForest reports that such field-aligned fluxes are not at all uncommon and, although statistics on the occurrence of those fluxes are not yet available, they seem to appear at nearly all local times.

The existence of an anisotropic flux distribution means that large fluxes of energetic particles can sometimes find their

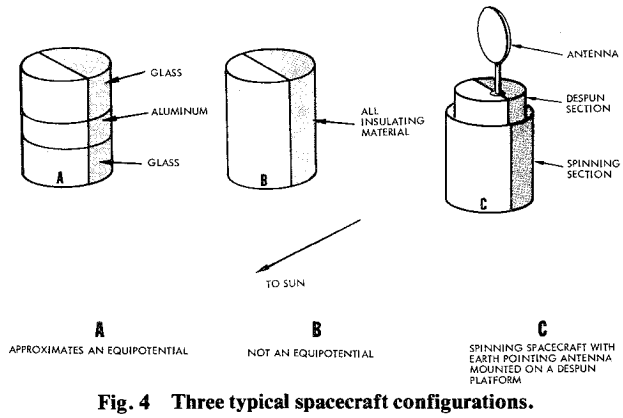

Fig. 4 Three typical spacecraft configurations.

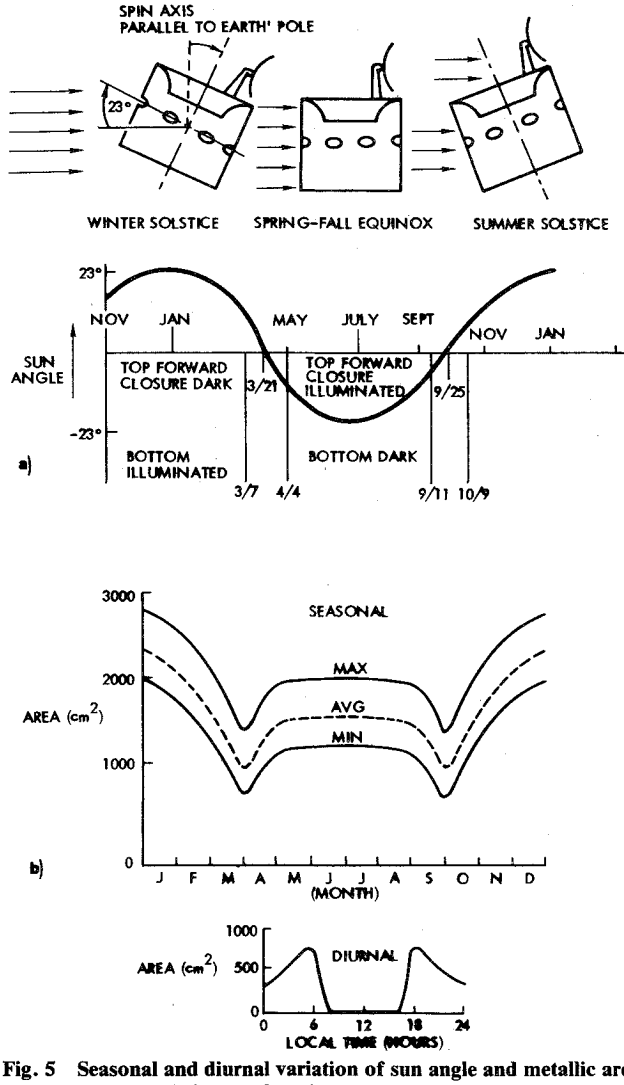

Fig. 5 Seasonal and diurnal variation of sun angle and metallic area exposed to sun. a) Seasonal variation of sun angle with respect to satellite equator. b) The diurnal and seasonal variation of metallic surface area exposed to the sun.

way into the ends of a spacecraft aligned with the Earth's axis of rotation. In addition, there is an increased possibility of differential charging between portions of the spacecraft.

Equivalent Circuit Components Associated with Spacecraft

Spacecraft configurations typical of satellites placed at synchronous altitudes, a region that is particularly subject to substorm phenomena, are shown in Fig. 4. The geometry shown in Fig. 4a is a cylindrical spacecraft with an aluminum belly

band (conductor) around its equator, and glass covered solar panels (dielectrics) above and below. Thus, when illuminated, the belly band can emit photoelectrons from its subsolar surface, and, due to the high conductivity of aluminum, it will be equipotential around its entire circumference, at the low (few volts negative) voltage determined by photoelectric emission currents. The dielectric portions, on Figs. 4a and 4b, can assume any potential between this subsolar value of several volts negative, down to a value $\phi \sim -E_e = kT_e \sim$ several kilovolts as one proceeds around to the antisolar line.[15]

The satellite shown in Fig. 4c consists of a spinning section with spin axis parallel to the Earth's axis of rotation, and a despun platform with an Earth-pointing antenna used for communication purposes. The satellite is maintained in a stationary position with respect to the Earth (at a fixed longitude). For such a satellite, the illumination on its surface undergoes three types of oscillations; a periodic oscillation at the spin frequency of the satellite; a diurnal oscillation of the despun section; and a seasonal variation as illustrated in Fig. 5a. Figure 5b shows the seasonal and diurnal variation in the metallic surface area illuminated by the sun, for a typical spacecraft in this configuration.

The photoelectron flux from a surface in sunlight in space has been found to be a strong function of the property of the surface. Few measurements of the flux have been made, and these were indirectly deduced from overall spacecraft charging rates. For conductors, Whipple[9] in 1965 measured a photoelectric current density from aluminum as $I = 3 \times 10^{-9}$ A/cm^2. On ATS-5, a spacecraft that is almost completely covered with dielectric material (thermal insulation and solar cells), DeForest has obtained a current density of $I = 8.2 \times 10^{-10}$ A/cm^2.[15] These fluxes are for plane surfaces normal to the sun. The geometry of the spacecraft must be considered in any actual application. For example, the average flux per unit area from the surface of a rotating unit cylinder whose axis is at right angles to the sun line would be approximately 25% of the above numbers.

Response of Spacecraft Charging Model to Geomagnetic Substorm

The response of a spacecraft charging model to a geomagnetic substorm was calculated by Inouye.[16] This model incorporated the effects of photoemission, secondary emission, and backscatter, which reduce the net electron charging rate, and effect material properties such as dielectric constants and resistivities.

An example of a simplified circuit assuming a step function representation of the substorm current is shown in Fig. 6. C_1 and C_2, both 2 μF, are the dark and illuminated capacitors, respectively, both having zero leakage conductance. For the spacecraft configuration shown in Fig. 4c, during the equinox season, C_2 is comprised mainly of the solar array cover glass. At equinox the surface materials on both the forward and bottom closures are parts of C_1. During the summer months, the forward closure surface is illuminated and becomes a part of C_2, while the bottom closure is dark. The seasonal and diurnal variation of illumination and the resulting photoemission from both dielectric and metallic surfaces affects the differential potentials generated as a result of substorm activity. The substorm plasma is represented by a -10 kV battery, which feeds the dark capacitor and structure through resistors which limit initial currents to 100 μA and 5 μA, respectively. The photoemission current generator incorporates diodes to limit currents to a single polarity and a resistor to reduce currents to zero for positive voltages greater than 2 V. The response shown in the lower portion of Fig. 6 shows the initial rapid rise, in the order of 100 sec, of both V_0 and V_1, in which the peak value of V_0 relative to V_1 is determined by the capacitive divider ratio C_2/C_1+C_2. Over a longer period, in the order of 10^4 sec, V_0 returns back to zero volts due to the photoemission current I_{photo}. The differential voltage stress $V_0 - V_1$ reaches its maximum value over this longer time constant period. The conditions described here are approximately

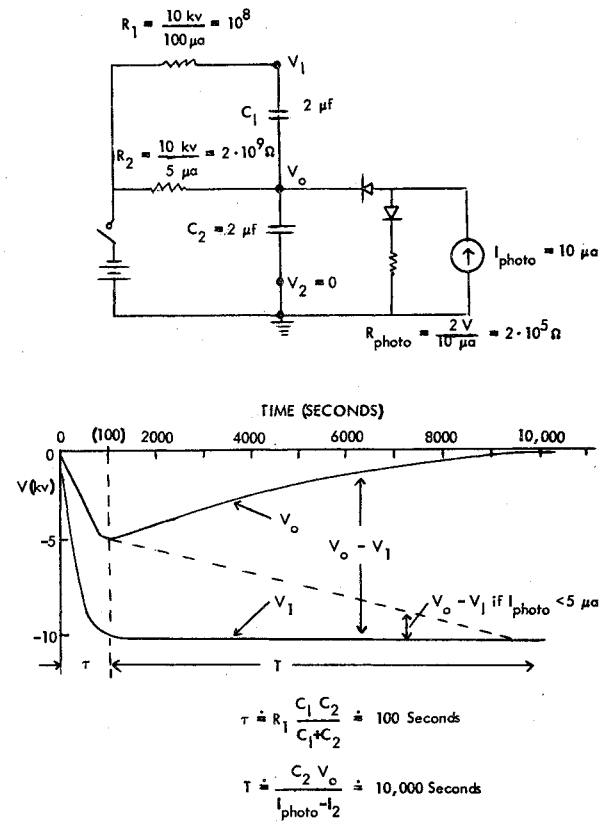

Fig. 6 Equivalent circuit of a simplified spacecraft configuration.

those which were obtained during the winter season for the spacecraft configuration shown in Fig. 4c, 5a, and 5b. Reduction of I_{photo} below 5μA, by changing the ratio of metallic to insulator surface area exposed to the sun, results in a voltage V_1, represented by the dotted line in Fig. 6. Such an analysis could, therefore, lead to the selection of surface materials for the reduction of voltage stress levels at locations most susceptible to RFI.

Observations of High Voltage Differential Charging and Correlation with Substorm Phenomena

The sequence of events to account for anomalous behavior of spacecraft consists of 1) the immersion of a spacecraft in a substorm plasma, 2) the differential charging of component parts of the spacecraft to a high voltage, 3) the generation of a vacuum arc when the voltage stress level exceeds the breakdown potential of the material, 4) the irradiation of selected spacecraft assemblies by the EMI waves associated with the vacuum arc, and finally 5) the induction of a transient pulse into the circuit of sufficient magnitude to activate the circuit or burn out some of its components. Verification of all these steps has been obtained either directly, through in-flight observation, or indirectly through ground observations, by correlating the anomalous event with the substorm. The most complete in-flight data verifying steps 1 and 2 of the process are obtained from the ATS-5 and ATS-6 satellites. There are numerous additional spacecraft measurements that verify the spacecraft charging phenomena (see, for example, Ref. 2).

To the best of our knowledge there has been only one in-orbit observation of vacuum arcing (step 3) directly related to substorms. In-orbit data verifying steps 4 and 5 are generally not available because of the lack of in-flight housekeeping monitors for charging/discharging phenomena. A large body of indirect evidence is, however, available that correlates the anomalous events with magnetic substorms. The indirect evidence has been obtained in two ways. First, by correlating the event with monitors on the Earth that measure the occurrence of a substorm at synchronous altitudes, and,

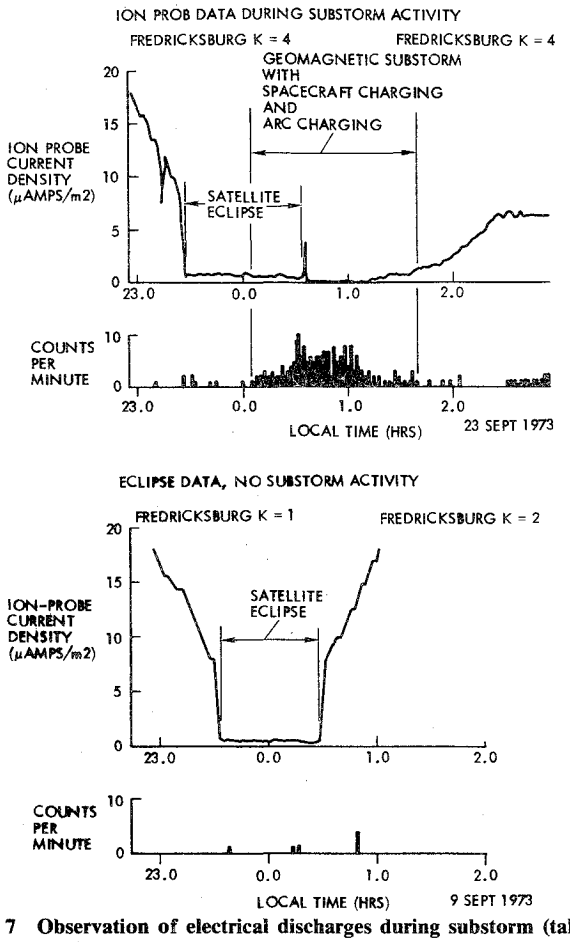

Fig. 7 Observation of electrical discharges during substorm (taken from Ref. 17).

secondly, by laboratory tests that simulate the malfunction of the given spacecraft component by irradiation with corona and arc discharge generated RFI.

In-Flight Observations

Observations of spacecraft charging were published by DeForest[15] and Whipple, et al.[11] DeForest measured the spacecraft potential developed during injection of energetic electrons ($3 \leq E_e \leq 20$ keV) into the local morning sector at 6.6 R_e. The potential of the spacecraft with respect to the plasma could be determinded by the distortion of the energy spectra of electrons and protons in the range 0.05-50 keV. The peaked proton distribution leads to the conclusion that the pre-eclipse distribution functions were translated *en mass* by a fixed voltage of 4.2 kV, with electrons retarded by this voltage and protons accelerated by it. This event was observed during a substorm-associated electron injection with mean energies $E_e = kT_e = 5$ keV and $E_p = kT_e = 10$ keV. The mean number density was ~ 1 cm^{-3}. This result can be explained by invoking a spacecraft voltage of -4.2 kV relative to plasma ground during eclipse, and a very much smaller spacecraft voltage relative to plasma ground when ATS-5 was illuminated (pre-eclipse). Such a picture is entirely consistent with the concept of such a spacecraft acting as a capacitive, floating Langmuir probe immersed in a hot, collisionless, tenuous plasma of $kT_e \sim 1$-10 keV.

DeForest made a detailed analysis of this Langmuir probe action using an idealized geometry of ATS-5 and taking into account the bombardment of the spacecraft surface by the injected keV electrons, the secondary emission electrons produced by these energetic primaries, and the photoelectron emission produced by solar photons when the spacecraft is illuminated. The results of this analysis indicated that the illuminated spacecraft surfaces were prevented by photoelectric emission from coming to more than a few hundred volts negative when bombarded by substorm-associated electrons. On the other hand, the eclipsed condition allows the spacecraft potential to reach almost the full value $\phi \sim E_e = kT_e$.

Observation of Electric Discharges

The observation of electrical discharges caused by satellite charging was reported by Shaw[17] and Cauffman and Shaw.[8] The detector consisted of a Langmuir probe, biased at -5.6 V with respect to the satellite frame. It was coupled to the telemetry so that the total current to the surface (dc-coupled channel) as well as pulses induced into the detector by electrical discharges (ac-coupled channel) could be measured. A particularly interesting example of increased pulse rates correlated with the observation of a substorm is shown in Fig. 7. At the bottom of the figure the probe current drops to nearly zero when the sensor is eclipsed. Only a few discharges are observed from the ac-coupled channel. The top part of the figure shows a similar eclipse of the sensor during a geomagnetic substorm. The plasma electrons now dominate the ion probe current and only after the elapse of over an hour does the ion probe current assume values more characteristic of the photoelectric current. The discharge rate is seen to be exceedingly high during the time that the probe is in eclipse and as it goes out of eclipse.

Indirect Observations

The effects of substorms are observed and measured on the ground by high latitude geomagnetic observatories. The perturbations in the geomagnetic field and the morphology of the visual aurora as measured by all-sky cameras provide the most extensive body of data on substorms. An excellent review of this work is found in an article by Rostaker.[18]

In terms of surface magnetic field variations, a substorm appears as a definite signature in the field components. It is hypothesized that the perturbation observed on the Earth is a crude measure of the dynamics of a substorm injection which occurred at 6.6 *Re*, provided both the observer and the injection occur on the same magnetic tube of force. If a spacecraft malfunction occurs at a time when there are perturbations on the tube of force on which the spacecraft is located, then it is likely that a substorm was in progress at the time of the malfunction. In the absence of more direct data one may establish that the substorm is at least a likely cause of the malfunction by attempting to find a correlation between the location of the satellite, the location of a distrurbed substorm condition, and the occurrence of a spacecraft malfunction.

Some examples of commonly observed circuit malfunctions on operational satellites are spontaneous firing of reset generator assemblies (RGA) that control the position of antennas, tunnel diode amplifier logic (TDAL) that controls the gain of an amplifier in a communication network, spin-up anomaly commands that spontaneously command the satellite to spin up, and converter switching anomalies that spontaneously switch from one power converter to a redundant unit on the same satellite.

There have been many examples of correlations of anomalous events with ground observations. Some of these have been described previously.[2,3,5,7] In a paper presented by Inouye,[16] the correlation coefficients obtained for the various events varies from close to 100% to practically zero. For example, all the RGA events were observed to occur in the midnight to dawn local time sector, during times of enhanced magnetic activity. TDAL and convector switching events were only marginally correlated with magnetic indices and ground station magnetograms, and did not seem to be preferentially distributed in the midnight to dawn local time sector.

Spacecraft Anomalies Observed Outside Midnight to Dawn Sector

There have been a large number of anomalies that do not seem to be well correlated with ground observations. Time

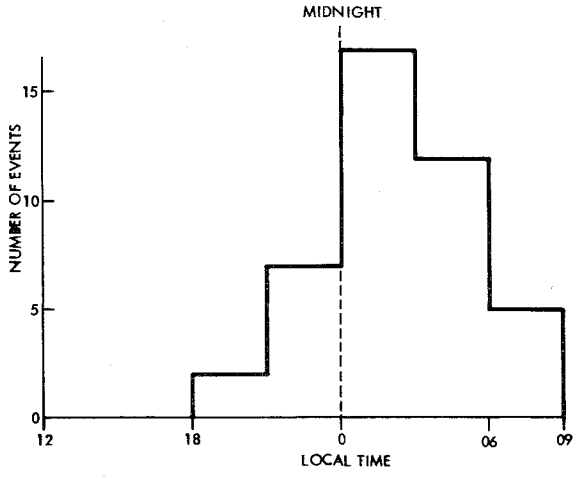

Fig. 8 Local time distribution of plasma dropouts at synchronous orbit, observed by UCSD spectrometer on ATS 5 during 1972.

delays associated with the spacecraft charging model could account for the lack of correlation, however, the existence of such time delays has not been verified. There are a number of other possible explanations ranging from the possibility that these events are not related to the environment to the possibility that another environmental phenomenon is the underlying cause.

Rostoker, DeForest, and McPherron[7] performed a study of other possible environmental phenomena in addition to the substorm to account for circuit anomalies on spacecraft. One candidate environmental transient, the so-called "plasma dropout" effect, would subject a spacecraft to a lower energy ambient plasma condition within seconds. Such transitions have been observed at ATS-5 and have been reported in the literature.[19] The ATS-5 data, recorded during 1972, were examined and 43 such events were identified. The local time distribution of the events is shown in Fig. 8. Since it is clear from Fig.8 that the plasma dropouts occur in the midnight to dawn sectors, similar to substorm injection events, it is unlikely that this mechanism could account for anomalies observed outside this time sector.

Other peculiarities of the plasma environment at synchronous orbit include the extremely rare crossing of the magnetopause observed during intense magnetospheric storm activity, and plasma flows associated with large amplitude micropulsation activity. Both of these unusual changes in the plasma environment at synchronous orbit are rare compared with the observation of circuit anomalies, on the defense communication satellites, for example.

The last candidate for environmental changes which may influence the occurrence of spacecraft charging is the encounter of a spacecraft with a detached region of cold plasma.[20] Such a plasma would be particularly effective in discharging the spacecraft. Differential potentials could arise if portions of the spacecraft are discharged with different time constants.[16]

Design of Spacecraft

The basic approach to reduce or eliminate the susceptibility of a spacecraft to substorm arcing malfunctions is to eliminate all capacitive configurations that can accumulate charge from the environment by either grounding or strapping the proper elements, and shielding circuits so as to reduce their susceptibility to arc-generated EMI. In addition, it is possible to reduce environmentally induced voltage stress levels at specific locations by selecting the proper surface materials and by closure of apertures and slits on the surface. The design requirements and criteria to conform to these improvements are given in Table 1. Three recommendations

Table 1 General design requirements and criteria

1) Shielding:	
	Provide adequate shielding for expected electric field levels and spectra
	Provide adequate shielding of cabling and connectors
	Use twisted pair wiring and common-mode rejection techniques where necessary
2) Grounding:	
	Ground all boxes to platform
	Ground cable shielding as frequently as possible
	Provide good grounds to structure for all metallized layers in thermal blankets.
	Ground all isolated or insulated metal structures, e.g., the aluminum honeycomb in the solar cell panels
3) Circuit design:	
	Each interbox wire should be grounded at each box for frequencies higher than the intended purpose for that wire.
	Filtering: circuits should be designed to minimize required bandwidths or maximize required rise-times on interbox wiring
4) Charge balance:	
	Reduce voltage stress levels at specific locations as determined by circuit susceptibility by selecting the proper surface material and ratio of conductor to insulator
5) Apertures and slits:	
	Close off all apertures and slits to reduce voltage stress levels at specific locations.
6) General:	
	Perform verification testing to assure the integrity of grounds, shields, circuit design, and charge balance
	Include high-intensity, high-frequency (arc discharge) sources in spacecraft EMI analyses. Once this is done properly, standard EMI problem-solving techniques may be brought to bear on each problem area.
	Minimize exposed insulated surface areas to reduce the occurrence of dielectric-to-metal arcs, e.g., use grounded conductive coating on solar cells and exposed mylar thermal blanket surfaces

follow from the various analyses performed and the observations outlined in previous sections:

1) Specific design, fabrication, and test procedures are recommended to reduce the vulnerability of spacecraft to substorm related malfunctions or failures. 2) A definitive laboratory test program is recommended to a) study the response of materials, components, and assemblies to charge buildup and arc breakdown, b) experimentally establish the interaction and the mechanism for the substorm induced anomaly, and c) provide a quantitative basis for designing future spacecraft so as to eliminate their susceptibility to substorm related phenomena. 3) The housekeeping data system of every operational spacecraft at synchronous altitude should carry simple monitors to determine substorm induced noise (RFI) and potential differences.

Spacecraft Test Program

Having adhered to the design criteria presented in Table 1, a spacecraft test verification program is recommended to eliminate or reduce all capacitive configurations and to assure that the spacecraft circuitry is not susceptible to arc generated RFI. The following spacecraft test program is recommended: 1) analysis of spacecraft configuration for unintentionally floating surfaces, e.g., mirrors, small pieces of inaccessible thermal blankets. 2) Verification of grounded and ungrounded surfaces and search for unintentionally floating components with appropriate detectors. An experimental search of all capacitive configurations should be undertaken.

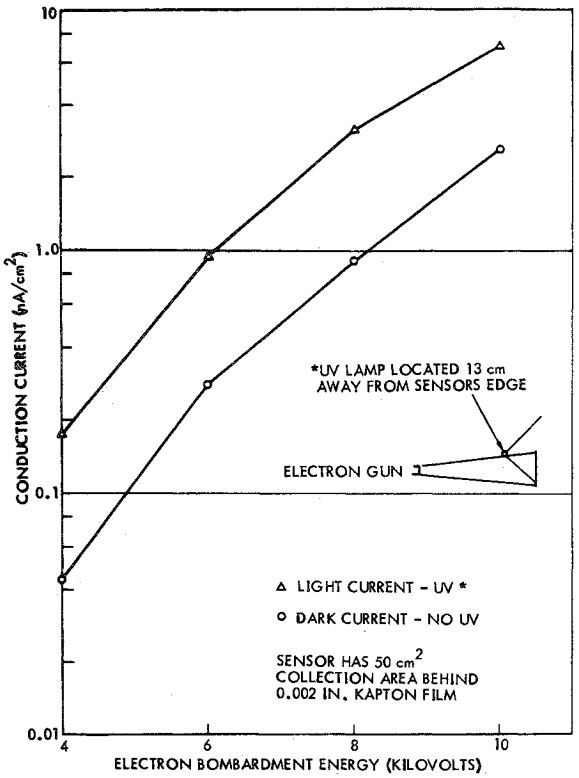

Fig. 9 Conduction current density through Kapton as function of incident electron bombardement voltage for uv absent and uv present conditions.

The capacitance and resistance of suspected configurations should be measured and recorded. 3) Verification of immunity to arc discharges with an arc discharge generator. The arc discharge generator, simulating the worse case expected environmental arcs, should be utilized in an integrated systems test to measure the susceptibility of the circuitry to substorm-related arc discharge phenomena.

Laboratory Program

The susceptibility of a spacecraft to high voltage differential charging depends, in part, on the selection of spacecraft materials and the dynamics of the arcing phenomena under standard environmental conditions. It is not possible to calculate voltage stress levels or to design a spacecraft so as to minimize these levels without knowledge of the bulk and surface resistivities of materials, the photoconduction magnitudes, the secondary emission ratios, and the photoemissive currents for both dielectrics and conductors. Unfortunately, some of these parameters have not been determined for the material commonly used in spacecraft design. For example, Hoffmaster and Sellen have measured the bulk resistivity of Kapton and find that the resistivity varies with the applied electric field stress level and light irradiation.[21,22] Figure 9 shows the nonlinear conduction current density throughout Kapton. The bulk resistivity of Kapton, under levels of electric stress from 0.1 to 1.6 megavolts/cm, were examined in both uv absent and uv present environments. For the most severe stress, resistivities of the order of 10^{14} Ωcm were observed, some four orders of magnitude lower than the nominally quoted figure of 10^{18} Ωcm bulk resistivity for Kapton.[21] When uv light at 2536 Å was directed on the sample, and for high stress, resistivity loss by another factor of 4 was observed.[22]

The incidence of photons on dielectric materials subjected to electron bombardment leads to charge deposition and transport processes that are more complicated than those same processes occurring in the absence of light.[22] Unfortunately, the data base for spacecraft materials is small at present, and additional laboratory measurements on bulk and surface resistivities, photoconduction magnitudes, secondary emission ratios, and photoemissive currents for both dielectrics and conductors are required. Potential equilibration measurements of individual materials and combined groups of materials under known environmental conditions should also be obtained. These joint experimental approaches will not only provide a data base for improved analyses but also show promise of delivering operational solutions to in-orbit charge-up problems.

Housekeeping Monitors

Every operational spacecraft at synchronous altitudes should carry a simple harness noise monitor and charge accumulation detector as part of the housekeeping system. This detector would fulfill the requirement for additional definitive data relating to substorm-related events occurring on spacecraft, and would be useful in correcting design weaknesses in a generic family of spacecraft. The corrections would then be implemented on subsequent flights.

The outstanding difficulty in performing a definitive study of substorm-related anomalies is the lack of data on the charge and discharge state of the spacecraft as a function of time [steps (2-5) listed in the sequence of events that account for the anomalous behavior of spacecraft]. This lack exists in every spacecraft system for which substorm-related events have been identified, and explains why it took over a decade to find the problem. In the case of the DSCS satellite, a small number of different types of spurious events were analyzed and compared with ground station data that included indications of thousands of substorm events. The small number of spacecraft anomalies and the meater amount of housekeeping data relating to these anomalies led to results that were essentially inconclusive. Without minimal housekeeping data relating to conditions on the spacecraft, one must go through a very laborious and time-consuming process to obtain correlative and phenomenological evidence for substorm-related spacecraft arcing. The major obstacle to demonstrating a conclusive correlation is the lack of a statistically significant sample of spacecraft anomalies and/or spacecraft failures. It is neither practical nor feasible to wait until the number of failures is sufficiently large to yield a statistically significant data base. It is, therefore, recommended that the on-board housekeeping system of every operational spacecraft at synchronous altitude include within its complement of housekeeping monitors a harness noise monitor and high voltage charge accumulation monitor to determine the effects of the substorm environment on the spacecraft.

The advantages of such monitors are 1) problems on a spacecraft will be identified before they become sufficiently serious to cause component or spacecraft faiulures. (The low level threshold of the detector would permit correlation of smaller events with minor changes in housekeeping data.) 2) Problems that are peculiar to a given spacecraft could be identified and analyzed. 3) The data base that is generated would be relevant to the study of the effects of substorms on spacecraft and would permit a meaningful correlation with ground station observations and observations of other space systems. 4) The charge detection system is simple and places minimum constraint on operational systems.

References

[1]Rosen, A., "Spacecraft Charging: Environment Induced Anomalies," AIAA Paper 75-91, Washington, D.C., 1975.

[2]Fredricks, R.W. and Scarf, F.L., "Observations of Spacecraft Charging Effects in Energetic Plasma Regions," *Photon & Particle Interactions with Surfaces in Space,* Reidel, Dordrecht-Holland, 1973, pp. 277-308.

[3]Fredricks, R.W. and Kendall, D.W., "Geomagnetic Substorm Charging Effects on Defense Satellite Communication System-Phase

ii," TRW Systems Group, Redondo Beach, Calif., Rept. 09670-7032-RU-00, June 1973.

[4]Rosen, A., et al., "RGA Analysis: Findings Regarding Correlation of Satellite Anomalies with Magnetospheric Substorms, and Laboratory Test Results," TRW Systems Group, Redondo Beach, Calif., Rept. 09670-7020-RO-00, Aug. 1972.

[5]"Final Report, TDAL Gain State Analysis," TRW Systems Group, Redondo Beach, Calif., Rept. 09670-7040-RU-00, Oct. 1973.

[6]"Final Report, Performance Anonaly Flight 9431, June 2, 1973," TRW Systems Group, Redondo Beach, Calif., Rept. 24512-AR-006-01, August 1973.

[7]"Final Technical Report, Program 777 Anomaly Investigation for Satellites 9433 and 9434," TRW Systems Group, Redondo Beach, Calif., Rept. 0970-REP-050-01, March 1974.

[8]Cauffman, D.P. and Shaw, R.R., "Transient Currents Generated by Electrical Discharges," Aerospace Corp., El Segundo, Calif., SPL-74-(4409-04)-1, June 1974.

[9]Whipple, E.C., "The Equilibrium Potential of a Body in the Upper Atmosphere and in Interplanetary Space," Ph.D. thesis, Dept. of Physics, George Washington Univ., Washington, D.C., 1965.

[10]Whipple, E.C., "The Equilibrium Electric Potential of a Body in the Upper Atmosphere and in Interplanetary Space," NASA, 1965.

[11]Whipple, E.C., Warnock, J.M., and Winkler, R.H., "Effect of Satellite Potential on Direct Ion Density Measurements through the Magnetopause," *Journal of Geophysical Research*, Vol. 79, Jan. 1974, pp. 179-186.

[12]Sellen, J.M., Jr. and Komatsu, G.K., "Electrical Equilibration of Active and Passive Spacecraft in Magnetospheric Plasmas," TRW Systems Group, Redondo Beach, Calif., Rept. 14292-6084-RU-00, Jan. 1974.

[13]McIlwain, C.E., "Coordinates for Mapping the Distribution of Magnetically Trapped Particles," *Journal of Geophysical Research*, Vol. 66, 1961, p. 3681.

[14]DeForest, S.E. and McIlwain, C.E., "Plasma Clouds in the Magnetosphere," *Journal of Geophysical Research*, Vol. 76, June 1971, pp. 3587-3611.

[15]DeForest, S.E., "Spacecraft Charging at Synchronous Orbit," *Journal of Geophysical Research*, Vol. 77, Feb. 1972. pp. 651-659.

[16]Inouye, G.T., "Spacecraft Charging Model," *Journal of Spacecraft and Rockets*, Vol. 12, Oct. 1975, pp. 613-620.

[17]Shaw, R.R., "Geomagnetic Substorm Activity Study Final Report," Aerojet Electrosystems Co., Azusa, Calif., Rept. 5120, Feb. 1975.

[18]Rostoker, G., "Polar Magnetic Substorms," *Review of Geophysics*, Vol. 10, 1972, p. 157.

[19]Bogott, F.H. and Mozer, F.S., "ATS-5 Observation of Energetic Proton Injection," *Journal of Geophysical Research*, Vol. 78, Dec. 1973, pp. 8113-8118 and 8119-8127.

[20]Chappel, C.R., "Detached Plasma Regions in the Magnetosphere," *Journal of Geophysical Research*, Vol. 79, May 1974, pp. 1861-1870.

[21]Hoffmaster, D.K. and Sellen, J.M., Jr., "Electron Swarm Tunnel Measurements of Kapton Bulk Resistivity at High Electric Stress Levels," TRW Systems Group, Redondo Beach, Calif., Rept. 4351.3.74-39, Sept. 1974.

[22]Sellen, J.M., Jr., "Electrical Equilibrium of Conducting and Insulating Materials in the Presence of Energetic Electrons and Ultraviolet Light," TRW Systems Group, Redondo Beach, Calif., Rept. 4351.3.74-44, October 1974.